A qualitative explanation for this result is the following: starting from the ground-state equilibrium geometry, motion in the direction of Δ (toward the excited-state equilibrium geometry) reduces the energy gap between the neutral and ionic states, increasing their mixing and therefore increasing the magnitude of the transition moment. This result is expected to be qualitatively correct as long as the magnitude of the coupling between neutral and ionic basis states does not vary significantly with the vibrational coordinate of interest. It may not hold even qualitatively for the intermolecular donor–acceptor stretch due to the anticipated strong dependence of the coupling matrix element on donor–acceptor separation.

Molecular Geometry of Vanadyl–Adenine Nucleotide Complexes Determined by EPR, ENDOR, and Molecular Modeling[1a]

Devkumar Mustafi, Joshua Telser,[1b] and Marvin W. Makinen*

Contribution from the Department of Biochemistry and Molecular Biology, The University of Chicago, Cummings Life Science Center, 920 East 58th Street, Chicago, Illinois 60637.
Received December 23, 1991

Abstract: The interactions of the vanadyl ion (VO^{2+}) with the adenine nucleotides AMP, ADP, and ATP and the α,β-methylene analogue of ADP (AMP-CP) have been investigated by electron paramagnetic resonance (EPR) and electron nuclear double resonance (ENDOR) spectroscopy. By spectrometric titration of VO^{2+} in solutions of different VO^{2+}:nucleotide molar ratios near neutral pH, it was shown on the basis of the peak-to-peak amplitude of the −3/2 perpendicular EPR absorption feature that the stoichiometry of metal:ligand binding for ADP, AMP-CP, and ATP was 1:2. No evidence for the binding of AMP was observed. The proton ENDOR features of the $-CH_2-$ group of the terminal methylene-substituted pyrophosphate group in the $VO(AMP\text{-}CP)_2$ complex in 50:50 aqueous–methanol yielded electron–proton distances of 4.2 and 4.9 Å. This observation, together with the detection of ^{31}P superhyperfine coupling in EPR and ENDOR spectra, established that chelation of VO^{2+} occurs via the phosphate groups. Analysis of proton ENDOR features of $VO(ADP)_2$ and $VO(AMP\text{-}CP)_2$ complexes indicated the presence of only axially coordinated solvent in the inner coordination sphere with no equatorially bound solvent. Except for the absence of the $-CH_2-$ resonance features, the proton ENDOR spectrum of $VO(ADP)_2$ was identical with that of $VO(AMP\text{-}CP)_2$, including resonance features assigned to the nucleoside moiety, corresponding to electron–proton separations of 5.3 and 6.0 Å, respectively. The metal–proton resonances of the nucleoside moiety and of the two methylene protons of AMP-CP required that the two AMP-CP or ADP molecules bind to the vanadyl ion in a 2-fold symmetric manner in equatorial positions through the α and β phosphate oxygens. Only with the ENDOR determined metal–proton distances of 5.3 and 6.0 Å assigned to H(8) of the guanine base and to H(5′) of the ribose moiety, respectively, was a stereochemically acceptable conformation obtained by computer based torsion angle search calculations. The results of these calculations showed that (1) the orientation of the base with respect to the glycosidic C(1′)–N(9) bond was *anti*, (2) the conformation about the C(4′)–C(5′) bond was *gauche gauche*, and (3) the conformation about the C(5′)–O(5′) bond was *trans*. In $VO(ATP)_2$, proton ENDOR features characteristic of only axially bound water were observed, suggesting that the VO^{2+} was chelated via the terminal β and γ phosphate groups. The EPR and ENDOR results indicate that with all three nucleotides only [$VO(nucleotide)_2^{eq}(solvent)^{ax}$] species were formed.

Introduction

The interactions of nucleotides in biological systems, particularly ADP[2] and ATP,[2] require a divalent metal ion as a cofactor whereby the phosphate moiety of the nucleotide chelates the metal ion. To understand these processes, it is important to know the detailed molecular structure and geometry of metal–nucleotide complexes. However, the structures of only a few divalent metal complexes of ATP have been determined by X-ray crystallographic studies.[3] In the case of ADP, the only crystal structure that has been hitherto determined to atomic resolution is that of the monorubidium salt.[4] In solution, structures of metal–nucleotide complexes have been studied mainly by NMR methods.[5,6] In most NMR studies Mn^{2+} has been used as a paramagnetic ion to probe the conformation and binding of nucleotides in solution.[5a,c,6b] Structural data obtained by NMR methods depend primarily on measurements of the enhancement of the nuclear spin–lattice relaxation rate to estimate distances between magnetic nuclei and the paramagnetic metal ion. Since the relaxation rate is inversely proportional to the metal–nucleus distance raised to the sixth power, the NMR data are often not sensitive enough for precise assignment of the conformation of molecules in solution. Furthermore, from such NMR data it is often difficult to determine whether the resonance derives from a distinct conformer

(1) (a) This work was supported by a grant from the National Institutes of Health (GM 21900). (b) Postdoctoral trainee supported by a training grant from the National Institutes of Health (HL 7237). Present address: Department of Chemistry, Roosevelt University, 430 S. Michigan Avenue, Chicago, IL 60605.

(2) The following abbreviations are used: EPR, electron paramagnetic resonance; ENDOR, electron nuclear double resonance; hf, hyperfine; hfc, hyperfine coupling; rf, radiofrequency; PIPES, piperazine-*N*,*N*′-bis[2-ethanesulfonic acid]; AMP, adenosine 5′-monophosphate; ADP, adenosine 5′-diphosphate; ATP, adenosine 5′-triphosphate; AMP-CP, α,β-methyleneadenosine 5′-diphosphate; AMP-PCP, β,γ-methyleneadenosine 5′-triphosphate; AMP-CPP, α,β-methyleneadenosine 5′-triphosphate.

(3) (a) Kennard, O.; Isaacs, N. W.; Motherwell, W. D. S.; Coppola, J. C.; Wampler, D. L.; Larson, A. C.; Watson, D. G. *Proc. R. Soc. London, A* **1971**, *325*, 401–436. (b) Sabat, M.; Cini, R.; Haromy, T.; Sundaralingam, M. *Biochemistry* **1985**, *24*, 7827–7833. (c) Orioli, P.; Cini, R.; Donati, D.; Mangani, S. *J. Am. Chem. Soc.* **1981**, *103*, 4446–4452.

(4) Viswamitra, M. A.; Hosur, M. V.; Shakked, Z.; Kennard, O. *Nature* **1976**, *262*, 234–236.

(5) (a) Zetter, M. S.; Lo, G. Y.-S.; Dodgen, H. W.; Hunt, J. P. *J. Am. Chem. Soc.* **1978**, *100*, 4430–4436. (b) Bock, J. L. *J. Inorg. Biochem.* **1980**, *12*, 119–130. (c) Jarori, G. K.; Ray, B. D.; Rao, B. D. N. *Biochemistry* **1985**, *24*, 3487–3494.

(6) (a) Happe, J. A.; Morales, M. *J. Am. Chem. Soc.* **1966**, *88*, 2077–2078. (b) Cohn, M.; Hughes, T. R., Jr. *J. Biol. Chem.* **1962**, *237*, 176–181. (c) Tanswell, P.; Thornton, J. M.; Korda, A. V.; Williams, R. J. P. *Eur. J. Biochem.* **1975**, *57*, 135–145.

0002-7863/92/1514-6219$03.00/0

or from multiple conformational species that are rapidly interconverting on the NMR time scale.

The VO^{2+} ion has been shown to be an effective paramagnetic substitute for many divalent metal ions in metalloproteins[7] and metalloenzymes.[8] Here we describe the coordination geometry of metal–adenine nucleotide complexes determined by electron paramagnetic resonance (EPR[2]) and electron nuclear double resonance (ENDOR[2]) spectroscopic methods, using the vanadyl ion (VO^{2+}) as a paramagnetic probe. The VO^{2+} ion, like Mn^{2+},[9] is characterized by narrow EPR signals over a wide range of temperatures and conditions. However, VO^{2+} has two major advantages over Mn^{2+}. Firstly, the EPR signal intensity is proportional only to bound VO^{2+} since at neutral pH free VO^{2+} forms an EPR-silent, polymeric $VO(OH)_2$ species.[10] Thus, the stoichiometry of metal–ligand binding can be determined by titrating VO^{2+} with ligand, using the EPR signal intensity to monitor the concentration of bound VO^{2+}. Secondly, the axial character of the vanadyl ion[11] allows one to assign by ENDOR the spatial disposition of coordinating ligands as equatorial or axial, a circumstance that is not possible with isotropic systems such as the Mn^{2+} ion. On this basis we determine the coordination geometry of ADP and ATP complexed to VO^{2+} by employing a stratagem[12] of ENDOR spectroscopy for selection of molecular orientation based on the axial and perpendicular components of the g matrix of the VO^{2+}. The results show that VO^{2+} is coordinated only by the phosphate groups of ADP and ATP, similar to that expected for Mg^{2+} complexes,[6a,b] and no coordination to atoms of the nucleic acid base is detected, in contrast to complexes formed with other divalent metal ions.[13]

Experimental Section

Chemicals. Vanadyl sulfate hydrate and methanol (99.9% spectrophotometric grade) were purchased from Aldrich Chemical Company, Inc. (Milwaukee, WI 53233); D_2O (99.8 atom % D), NaOD (>99 atom % D), PIPES, the disodium salt of ATP, AMP-PCP and AMP-CPP, and the sodium salts of AMP, ADP, and AMP-CP from Sigma Chemical Company (St. Louis, MO 63178). The deuterated compounds CD_3OD (99.8 atom % D), CD_3OH (99 atom % D), CH_3OD (99 atom % D), and DCl (99 atom % D) were obtained from Cambridge Isotope Laboratories, Inc. (Woburn, MA 01801).

Methods. Solutions of vanadyl–nucleotide complexes were prepared by mixing together the desired quantity of the nucleotide in 0.03 M PIPES buffer at pH 6.5 with vanadyl sulfate in a small quantity of H_2O or D_2O under a nitrogen atmosphere and adjusting the pH to 6.5 with HCl (or DCl) or NaOH (or NaOD). For EPR and ENDOR studies, the final metal ion concentration was 10 mM while the nucleotide concentration varied from 0 to 100 mM. Methanol was then added to yield a final 50:50 (v/v) cosolvent mixture. All solutions were purged with nitrogen gas and stored frozen in EPR sample tubes to prevent oxidation.

EPR and ENDOR spectra were recorded with an X-band Bruker ER200D spectrometer equipped with an Oxford Instruments ESR10 liquid helium cryostat and a Bruker digital ENDOR accessory, as previously described.[12,14] Typical experimental conditions for EPR measurements were the following: sample temperature, 20 K; microwave frequency, 9.46 GHz; incident microwave power, 64 μW; frequency modulation of the rf field, 12.5 kHz; field modulation amplitude, 0.8 G. Conditions for ENDOR measurements include the following: microwave power, 6.4 mW; rf power, 70 W. In general, a frequency modulation depth of the rf field of no more than 30 kHz was used to record ENDOR spectra. Under identical conditions but with 15-kHz modulation, the spectra did not differ in line shape and showed only much reduced peak-to-peak amplitudes. No modulation of the static laboratory magnetic field was used for recording ENDOR spectra.

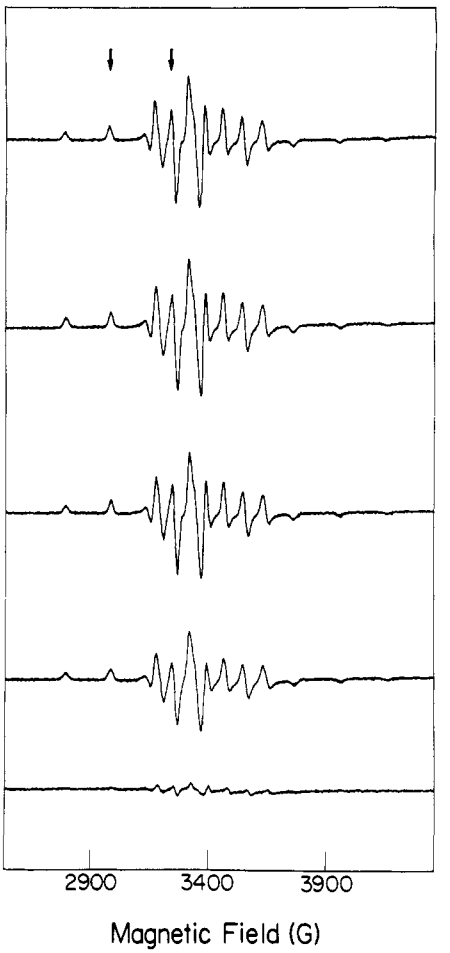

Figure 1. First-derivative EPR absorption spectra of VO^{2+}–ATP complexes in frozen solutions of an aqueous–methanol (50:50 v/v) cosolvent mixture. The solutions were buffered to pH 6.5 with 0.03 M PIPES. The spectra were recorded under identical spectrometer settings with different VO^{2+}:ATP molar ratios of 1:10.0, 1:7.5, 1:4.0, 1:1.8, and 1:0.4 from top to bottom, respectively, at a final metal ion concentration of 0.01 M. The −5/2 parallel (~3000 G) and −3/2 perpendicular (~3270 G) EPR absorption features, saturated for ENDOR studies, are indicated by arrows.

Molecular Modeling. Molecular modeling of the structures of nucleotide complexes of the VO^{2+} ion was carried out with use of the programs FRODO,[15] INSIGHT,[16] and SYBYL[17] running on an Evans and Sutherland PS390 molecular graphics terminal. The atomic coordinates of the non-hydrogen atoms of ATP were taken from the X-ray defined structure of the disodium salt of ATP.[3a] The molecular model of ADP was constructed by deleting the terminal PO_3 group from the coordinate listing of ATP. The structure of AMP-CP was constructed by substituting the P–O–P fragment of ADP with P–CH_2–P using the P–C bond lengths of 1.790 and 1.794 Å and the P–C–P valence angle of 117.2° in

(7) (a) Chasteen, N. D.; DeKoch, R. J.; Roggers, B. L.; Hanna, M. W. *J. Am. Chem. Soc.* **1973**, *95*, 1301–1309. (b) Chasteen, N. D.; Francavilla, J. *J. Phys. Chem.* **1976**, *80*, 867–871. (c) White, L. K.; Chasteen, N. D. *J. Phys. Chem.* **1979**, *83*, 279–284.

(8) (a) DeKoch, R. J.; West, D. J.; Cannon, J. C.; Chasteen, N. D. *Biochemistry* **1974**, *13*, 4347–4354. (b) Chasteen, N. D. *Structure Bonding (Berlin)* **1983**, *53*, 105–138.

(9) (a) Chapman, B. E.; O'Sullivan, W. J.; Scopes, R. K.; Reed, G. H. *Biochemistry* **1977**, *16*, 1005–1010. (b) Reed, G. H.; Leyh, T. S. *Biochemistry* **1980**, *19*, 5472–5480. (c) Reed, G. H.; Markham, G. D. In *Biological Magnetic Resonance*; Berliner, L. J., Reuben, J., Eds.; Plenum: New York, 1984; Vol. 6, pp 73–142.

(10) Francavilla, J.; Chasteen, N. D. *Inorg. Chem.* **1975**, *14*, 2860–2862.

(11) (a) Gersmann, H. R.; Swalen, J. D. *J. Chem. Phys.* **1962**, *36*, 3221–3233. (b) Albanese, N. F.; Chasteen, N. D. *J. Phys. Chem.* **1978**, *82*, 910–914.

(12) Mustafi, D.; Makinen, M. W. *Inorg. Chem.* **1988**, *27*, 3360–3368.

(13) (a) Goodgame, D. M. L.; Jeeves, I.; Reynolds, C. D.; Skapski, A. C. *Nucl. Acids Res.* **1975**, *2*, 1375–1379. (b) Gilbert, R. W.; Bau, R. In *Metal Ions in Biological Systems*; Sigel, H., Ed.; Marcel Dekker: New York, 1979; Vol. 8, pp 1–55. (c) Pezzano, H.; Podo, F. *Chem. Rev.* **1980**, *80*, 366–401.

(14) Yim, M. B.; Makinen, M. W. *J. Magn. Reson.* **1986**, *70*, 89–105.

(15) (a) Jones, T. A. In *Computational Crystallography*; Sayre, D., Ed.; Clarendon Press: Oxford, 1982; pp 303–317. (b) Jones, T. A. *Methods Enzymol.* **1985**, *115*, 157–171.

(16) Dayringer, H. E.; Tramontano, A.; Sprang, S. R.; Fletterick, R. J. *J. Mol. Graphics* **1986**, *4*, 82–87.

(17) (a) Marshall, G. R., personal communication. Detailed information on the use of this program package can be obtained from Tripos Associates, Inc., 1600 S. Hanley Road, St. Louis, MO 63144. (b) Naruto, S.; Motoc, J.; Marshall, G. R.; Daniels, S. B.; Sofia, M. J.; Katzenellenbogen, J. A. *J. Am. Chem. Soc.* **1985**, *107*, 5262–5270. (c) Iijima, H.; Dunbar, J. B., Jr.; Marshall, G. R. *Proteins: Struct., Funct., Genet.* **1987**, *2*, 330–339.

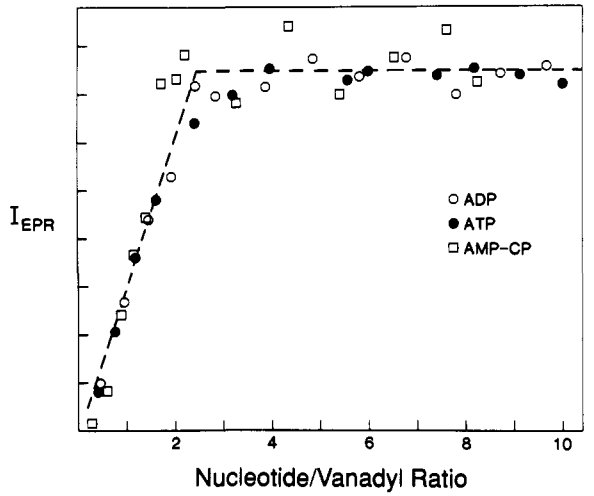

Figure 2. EPR spectrometric titration of the VO^{2+} ion complexed to ADP, ATP, and AMP-CP. The EPR signal intensity for the −3/2 perpendicular line of the VO^{2+} ion binding to nucleotides is plotted as a function of nucleotide:vanadyl ratio. Dashed lines are drawn through the experimentally measured points. The data for AMP-CP exhibit greater noise because lower VO^{2+} concentrations were used to conserve this expensive synthetic nucleotide.

methylenediphosphonic acid.[18] Positions of hydrogen atoms were calculated on the basis of idealized valence angles and C–H bond lengths of 1.08 and 1.045 Å for sp^3 and sp^2 hybridized carbons, respectively, and 1.00 Å for hydroxyl oxygens as previously described.[12,19] The V=O bond length of 1.59 Å determined by X-ray diffraction studies[20] was used for molecular modeling.

Results and Discussion

A. EPR of VO^{2+}–Nucleotide Complexes. 1. Stoichiometry of Vanadyl–Nucleotide Binding. In the V^{4+} ion with a $3d^1$ configuration, the unpaired electron is strongly coupled to the ($I = {}^7/_2$) ^{51}V nucleus. In frozen solution, the VO^{2+} ion is characterized by an axially symmetric **g** matrix and exhibits eight parallel and eight perpendicular absorption lines. Figure 1 illustrates the EPR absorption spectra of VO^{2+}–ATP complexes in aqueous–methanol cosolvent mixtures. A change in the relative peak-to-peak amplitude was observed only at metal:nucleotide molar ratios less than 1:2. Similar results were observed with ADP and AMP-CP as the ligating nucleotide. Comparable changes in the peak-to-peak amplitudes were also observed for VO^{2+}–nucleotide complexes in frozen aqueous solutions without added methanol. However, ENDOR resonances could be detected only for VO^{2+}–nucleotide complexes in frozen glassy solutions of methanol–water mixtures.

Figure 2 illustrates a plot of the peak-to-peak amplitude of the −3/2 perpendicular EPR absorption feature for varying vanadyl:nucleotide ratios. The −3/2 perpendicular resonance feature was selected to monitor the stoichiometry of nucleotide binding since, in frozen solution, it is the second most intense signal and has virtually no overlap with nearby parallel EPR transitions. Francavilla and Chasteen have shown that the VO^{2+} ion loses EPR intensity in the absence of chelating agents over the pH range 5–11 due to formation of $VO(OH)_2$ which polymerizes and is EPR silent.[10] Therefore, at neutral pH, peak-to-peak amplitudes are proportional only to the amount of nucleotide-bound VO^{2+}. Figure 2 shows a linear increase in signal intensity up to a vanadyl:nucleotide ratio of 1:2, after which the signal intensity remains constant. The data indicate that the stoichiometry of vanadyl:nucleotide binding is 1:2 in the presence of excess nucleotide.

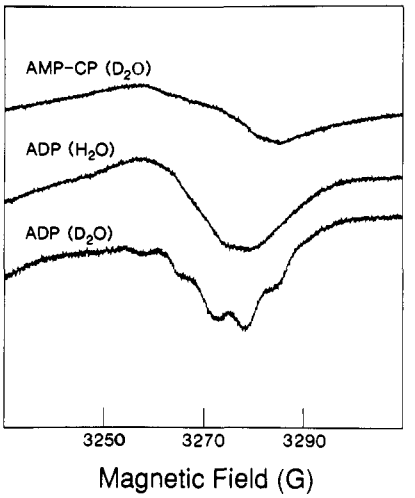

Figure 3. Line widths of the −3/2 perpendicular EPR absorption feature and ^{31}P superhyperfine structure for the VO^{2+} ion complexed to ADP and AMP-CP in frozen solutions of natural abundance and perdeuterated aqueous–methanol (50:50 v/v) cosolvent mixtures. The nucleotide:vanadyl ratio was in excess of 2:1.

Table I. Line Widths of the −3/2 Perpendicular EPR Absorption Feature for the VO^{2+} Ion Complex with Nucleotides in Frozen Solutions of Natural Abundance and Perdeuterated Water–Methanol Cosolvent Mixtures

complexing ligand	ΔH_{pp} (G)	^{31}P superhyperfine feature
H_2O	11.40 ± 0.13	
D_2O	5.65 ± 0.08	
ADP (H_2O)	22.51 ± 0.18	weakly resolved
ADP (D_2O)	21.96 ± 0.18	five well-resolved lines (a_p = 6.62 ± 0.08 G) with intensity ratio of 1:4:6:4:1
AMP-CP (H_2O)	26.65 ± 0.26	weakly resolved
AMP-CP (D_2O)	26.11 ± 0.25	five weakly resolved lines
ATP (H_2O)	23.84 ± 0.21	not resolved
ATP (D_2O)	23.31 ± 0.20	not resolved

In the case of AMP, addition of VO^{2+} at pH 6.5 resulted in formation of a large amount of precipitate, presumably the $VO(OH)_2$ polymer, at both low and high ratios of AMP to VO^{2+}. These results suggested that at neutral pH the vanadyl ion does not bind to the adenine or ribose moieties and that chelation of VO^{2+} occurs via the phosphate groups of ADP, AMP-CP, and ATP. We have also tested vanadyl:nucleotide binding with two methylene analogues of ATP. Under identical conditions of pH, a plateau in the signal intensity of the −3/2 perpendicular resonance feature appeared at a VO^{2+}:nucleotide ratio of ca. 1:3 for the β,γ-methylene analogue AMP-PCP. With the α,β-methylene analogue AMP-CPP, no plateau was observed even with VO^{2+}:AMP-CPP ratios greater than 1:6. These differences in metal binding behavior exhibited by the methylene analogs might be attributable to their altered ionization properties.[21a,b] However, since they bind divalent metal ions more tightly in comparison to ATP at both neutral and high pH,[21b,c] the origin of their altered binding behavior with respect to VO^{2+} is not clear. Conditions of higher pH were not examined because of the greater tendency of the vanadyl ion to polymerize and precipitate.[10]

2. Coordination Environment of VO^{2+} in Nucleotide Complexes. In view of the demonstrated stoichiometry of VO^{2+}:nucleotide binding in Figure 2, all further characterization of nucleotide-bound VO^{2+} refers to conditions of VO^{2+}:nucleotide concentrations of at least 1:4. In Figure 3 we illustrate the −3/2 perpendicular

(18) DeLaMatter, D.; McCullough, J. J.; Calvo, C. *J. Phys. Chem.* **1973**, *77*, 1146–1148.
(19) (a) Mustafi, D.; Sachleben, J. R.; Wells, G. B.; Makinen, M. W. *J. Am. Chem. Soc.* **1990**, *112*, 2558–2566. (b) Wells, G. B.; Mustafi, D.; Makinen, M. W. *J. Am. Chem. Soc.* **1990**, *112*, 2566–2574. (c) Joela, H.; Mustafi, D.; Fair, C. C.; Makinen, M. W. *J. Phys. Chem.* **1991**, *95*, 9135–9144.
(20) Ballhausen, C. J.; Djurinskij, B. F.; Watson, K. J. *J. Am. Chem. Soc.* **1968**, *90*, 3305–3309.
(21) (a) Myers, T. C.; Nakamura, K.; Flesher, J. W. *J. Am. Chem. Soc.* **1963**, *85*, 3292–3295. (b) Yount, R. G.; Babcock, D.; Ballantyne, W. M.; Ojala, D. *Biochemistry* **1971**, *10*, 2484–2489. (c) Yount, R. G. *Adv. Enzymol.* **1975**, *43*, 1–56.

absorption feature of the VO^{2+} ion complexed to ADP and AMP-CP in natural abundance and perdeuterated water–methanol cosolvent mixtures. In Table I we have summarized the peak-to-peak EPR absorption line widths of the −3/2 perpendicular feature of the VO^{2+} ion complexed with each of the three nucleotides in both solvents. Also listed in Table I are the corresponding line widths of the free VO^{2+} ion. For the solvated VO^{2+} ion, there is an approximate 5.75-G decrease in the line width of the −3/2 perpendicular resonance absorption feature upon introduction of perdeuterated solvents.[12] This value is comparable to that of 6.15 G for the transfer of VO^{2+} ion from H_2O–glycerol to D_2O–glycerol mixtures.[11b] On the other hand, no significant decrease in line width was observed upon introduction of deuterated solvents in the case of VO^{2+}–nucleotide complexes. According to the analysis of Albanese and Chasteen,[11b] these results indicate that in the vanadyl–nucleotide complexes no solvent molecule is directly coordinated to the VO^{2+} ion in an equatorial position.

In Figure 3 the bottom spectrum shows the −3/2 perpendicular EPR feature of the VO^{2+} ion complexed to ADP in the presence of perdeuterated solvent. The underlying superhyperfine structure exhibits quintet features spaced at 6.32-G intervals with an approximate intensity ratio of 1:4:6:4:1. This pattern can be ascribed to four equivalent nuclei of $m_I = {}^1/_2$ interacting with the VO^{2+} ion and dominated by isotropic hf interactions. This magnitude of hf coupling can be ascribed only to the ($I = {}^1/_2$) ^{31}P nucleus. Since the isotropic hyperfine coupling constant of ^{31}P is large (~10178 MHz[22]), the 6.62 G (18.54 MHz) coupling corresponds to less than 0.2% of the unpaired spin density in a pure phosphorus 3s orbital.[23]

From the EPR spectrometric titration we have shown that the stoichiometry of metal:ligand binding is 1:2. Since the isotropic superhyperfine couplings of the four ^{31}P nuclei in the $VO(ADP)_2$ complex are equal, both phosphate groups of the two ADP molecules must be coordinated to the VO^{2+} ion such that all four phosphorus atoms are geometrically equivalent with respect to the metal center. For the $VO(ADP)_2$ complex in the natural abundance cosolvent mixture, this ^{31}P superhyperfine pattern is only weakly resolved. In natural abundance solvents, the couplings from solvent protons may broaden the EPR spectrum and, consequently, limit the resolution of the superhyperfine structure.[10-12] For the $VO(AMP\text{-}CP)_2$ complex, the methylene protons may also have a broadening contribution to the EPR spectrum, and as seen in Table I, the largest EPR line width was indeed observed for this complex. Nonetheless, in perdeuterated solvents, a weakly resolved five-line superhyperfine pattern was observed for this complex, as seen in the top spectrum of Figure 3. This observation indicates that the coordination of the VO^{2+} ion with the phosphate groups in $VO(AMP\text{-}CP)_2$ complex is similar to that in the $VO(ADP)_2$ complex.

For the $VO(ATP)_2$ complex, only a single, broad EPR line was observed, even in perdeuterated solvents. If all three phosphate groups bind with the VO^{2+} ion, a symmetrical pattern of hyperfine structure should be observed. Since the maximum stoichiometry of VO^{2+}:ATP binding was also found to be 1:2, we believe that the phosphate groups in ATP bind with the VO^{2+} ion such that the phosphorus atoms are non-equivalent with respect to the metal center. This arrangement would give distinct isotropic couplings for each ^{31}P atom, which in turn would yield a broad, unresolved EPR line. A more comprehensive description of the coordination geometry of the $VO(ATP)_2$ complex is given below.

B. ENDOR of VO^{2+}–Nucleotide Complexes. 1. Assignment of ENDOR Resonance Features. ENDOR spectroscopy is performed at fixed magnetic field strength $\mathbf{H}_0$ by observing the changes in the EPR signal intensity caused by nuclear transitions induced through sweeping the sample with an rf field. In the general case, the ENDOR transition frequencies are functions of the relative orientations of molecules with respect to $\mathbf{H}_0$, of the electron–nuclear dipolar separation, and of the relative orientations of the principal magnetic axes of the **g** matrix and the hf interaction matrix. For a system of low g anisotropy, as in the case of the VO^{2+} ion,[11] the first-order ENDOR transition frequencies $\nu_\pm$ within the strong-field approximation are given by eq 1. Here,

$$\nu_\pm = \nu_n \pm |A|/2 \quad (1)$$

$\nu_\pm$ represents the spacing of the pair of ENDOR features that appear symmetrically about the free nuclear frequency ν_n and A represents an orientation-dependent hf coupling. The EPR spectrum of VO^{2+} is dominated by the hf anisotropy of the vanadium nucleus. On the basis of the −5/2 parallel or the −3/2 perpendicular EPR absorption features, we select $\mathbf{H}_0$ for ENDOR so that the molecular z-axis coincident with the V=O bond is oriented parallel or perpendicular, respectively, to the static magnetic field.

Figure 4 illustrates the proton ENDOR spectra of the $VO(ADP)_2$ complex in natural abundance and perdeuterated cosolvent mixtures. The line pairs labeled S1 and S2 are assigned to solvent molecules because they are seen only in natural abundance solvents. Both line pairs are seen also for the VO^{2+} ion complexed

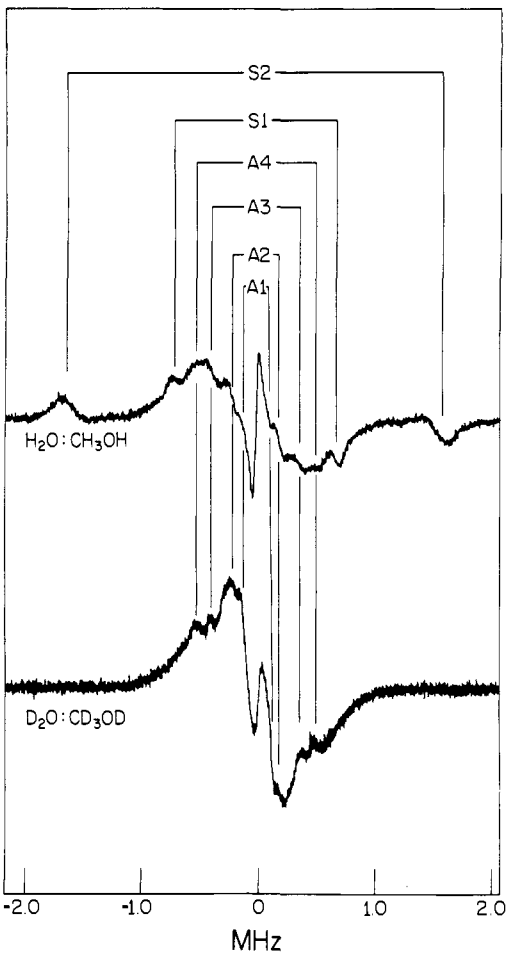

Figure 4. Proton ENDOR spectra of the $VO(ADP)_2$ complex in 50:50 H_2O:CH_3OH (top spectrum) and D_2O:CD_3OD (bottom spectrum) cosolvent mixture. The VO^{2+} complexes were prepared with a VO^{2+}:ADP molar ratio of 1:8, buffered to pH 6.5 with 0.03 M PIPES. For ENDOR spectra the static laboratory magnetic field was set to the −3/2 perpendicular EPR absorption line (~3270 G). The ENDOR absorption features are identified in the stick diagram and are equally spaced about the free proton frequency of 13.88 MHz. The line pairs denoted by symbols A and S belong to protons of the bound ADP moiety and to solvent molecules, respectively.

(22) Values of the isotropic hyperfine coupling constants of various nuclides are generally tabulated in standard textbooks, e.g.: Wertz, J. E.; Bolton, J. R. *Electron Spin Resonance*; McGraw-Hill: New York, 1979.

(23) Under conditions of VO^{2+}:ADP in excess of 1:2, we have observed only the quintet superhyperfine coupling pattern as shown in Figure 3. However, for solutions in which the VO^{2+}:ADP ratio was 1:1, the superhyperfine coupling due to ^{31}P was observed as a three-line pattern with an approximate 6.74 G splitting and an intensity ratio of 1:2:1. This pattern is indicative of two equivalent ^{31}P nuclei interacting with the VO^{2+} ion.

Table II. Observed Proton ENDOR Splittings of the VO^{2+} Ion Complex with AMP-CP, ADP, and ATP in Frozen Solutions of Water–Methanol Cosolvent Mixtures

H_0 Setting	line pair[a]	line splittings[b] (MHz)	assignment
−3/2 ⊥, −5/2 ∥	A1	0.24	ADP, AMP-CP
−3/2 ⊥, −5/2 ∥	A2	0.44	ADP, AMP-CP
−3/2 ⊥	A3	0.81	ADP, AMP-CP
−3/2 ⊥	A4	1.07	ADP, AMP-CP
−3/2 ⊥, −5/2 ∥	C1	0.44	AMP-CP
−3/2 ⊥, −5/2 ∥	C2	1.22	AMP-CP
−3/2 ⊥	C3	1.52	AMP-CP
−3/2 ⊥	C4	1.81	AMP-CP
−3/2 ⊥	S1	1.40	solvent (axial CH_3–)[c]
−3/2 ⊥	S2	3.13	solvent (axial OH)[c]

[a] Line pairs are assigned in Figures 4 and 5. Line pairs that are observed in the −5/2 parallel spectra are not shown. [b] Estimated uncertainty of the line splitting is ±0.01 MHz. [c] These line pairs for the solvent protons are seen in the ENDOR spectra of all three VO^{2+}–nucleotide complexes.

to AMP-CP or ATP in natural abundance cosolvent mixtures. On the basis of ENDOR spectra of VO^{2+}–nucleotide complexes in H_2O:CH_3OH, H_2O:CD_3OH, D_2O:CH_3OD, and D_2O:CD_3OD cosolvent mixtures, the line pair S1 is assigned to methyl protons of the solvent, and S2 is assigned to hydroxyl protons. These line pairs are seen with $\mathbf{H}_0$ at only the −3/2 perpendicular EPR absorption feature. With $\mathbf{H}_0$ at the −5/2 parallel EPR spectral component, two weak ENDOR absorptions with line splittings of 6.0 and 2.4 MHz are observed respectively for the hydroxyl and methyl protons of solvent molecules.

To assign the principal hfc components of these protons, we use the same stratagem as described previously in the ENDOR study of the solvation structure of the VO^{2+} ion.[12] Since the line pairs S1 and S2 for the methyl and hydroxyl protons, respectively, are seen only with $\mathbf{H}_0$ at the −3/2 perpendicular EPR feature, they are assigned to the perpendicular hfc components of protons of axially coordinated solvent molecules. If these features belonged to the perpendicular hfc components of equatorially located protons, they would then be observed with $\mathbf{H}_0$ settings at both the −3/2 perpendicular and −5/2 parallel EPR spectral components. Two weak resonance features with line splittings of 6.0 MHz for the hydroxyl protons and 2.4 MHz for the methyl protons, observed only with $\mathbf{H}_0$ at the −5/2 parallel EPR feature, are assigned to the parallel hfc components of axially coordinated solvent molecules. For VO^{2+}–nucleotide complexes, no ENDOR feature was observed for protons from equatorially coordinated solvent molecules. Thus, the ENDOR results are consistent with the EPR results, indicating that in VO^{2+}–nucleotide complexes no inner sphere coordinated solvent molecule is bound to the VO^{2+} ion in the equatorial plane.

In Figure 4 the resonance features labeled A1, A2, A3, and A4 are seen in both natural and perdeuterated cosolvent mixtures. These features must come, therefore, from nucleotide protons. In the ENDOR spectra, the line pairs A3 and A4 are seen only with $\mathbf{H}_0$ at the −3/2 perpendicular EPR feature while the line pairs A1 and A2 are seen with $\mathbf{H}_0$ at both the −3/2 perpendicular and the −5/2 parallel EPR features. Following the same strategem, we assign the line pairs A1 and A2 to perpendicular hfc components and A3 and A4 to parallel hfc components of nucleotide protons located in or very close to the equatorial plane. Figure 5 illustrates the proton ENDOR spectrum of the VO^{2+} ion complexed to AMP-CP. Since this spectrum was taken in a perdeuterated cosolvent mixture, all resonance features must belong to the nucleotide. In addition to the resonance absorptions labeled A1–A4, as observed for $VO(ADP)_2$ in a perdeuterated solvent, the features C1–C4 are observed and must, therefore, arise from the $-CH_2-$ group bridging the phosphorus atoms.

The values of ENDOR line splittings and their assignments for VO^{2+}–nucleotide complexes are listed in Table II. The line pairs A1, A2, A3, and A4 are seen in both the $VO(ADP)_2$ and the $VO(AMP\text{-}CP)_2$ complexes and are assigned to non-exchangeable protons of either the adenine or the ribose moieties. Three line pairs, labeled C2, C3, and C4, are seen only for the $VO(AMP\text{-}CP)_2$ complex; these features belong, therefore, to the methylene protons of AMP-CP. By comparing the ENDOR spectra of VO^{2+} ion complexed to ADP and AMP-CP in Figures 4 and 5, particularly with respect to the amplitude of the A2 resonance absorption, we assign an additional line pair to the methylene protons labeled C1. The line pairs C3 and C4 are seen only in ENDOR spectra with $\mathbf{H}_0$ at the −3/2 perpendicular EPR feature, and the line pairs C1 and C2 are seen at both the parallel and the perpendicular $\mathbf{H}_0$ settings of the EPR spectrum. Therefore, C1 and C2 are assigned to the perpendicular hfc components, and C3 and C4 to the parallel hfc components of the two methylene protons of AMP-CP. For the $VO(ATP)_2$ complex, ENDOR features can be assigned only to axially coordinated solvent, and no ENDOR feature characteristics of the nucleoside moiety was observed.

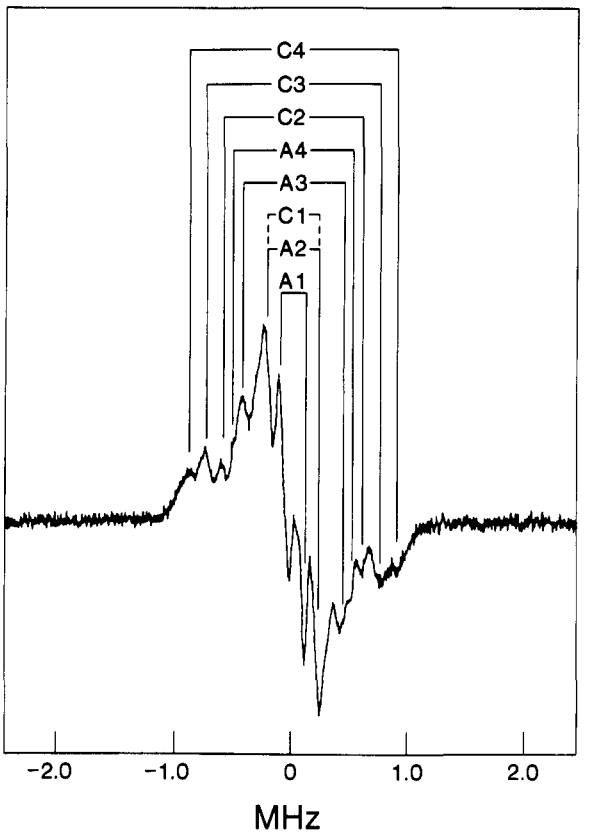

Figure 5. Proton ENDOR spectrum of the $VO(AMP\text{-}CP)_2$ complex in perdeuterated cosolvent mixtures. $\mathbf{H}_0$ was set to the −3/2 perpendicular EPR absorption line. The line pairs denoted by symbols C1, C2, C3, and C4 are from the methylene protons of AMP-CP. Other conditions are as in Figure 4.

In addition to several proton ENDOR features from solvent and vanadyl bound nucleotide molecules, we have also observed ^{31}P ENDOR features for all three VO^{2+}–nucleotide complexes. A broad ^{31}P matrix signal was observed at 5.7 MHz, due to distant ^{31}P nuclei. This matrix signal comes from unbound nucleotide molecules because it was observed only when the VO^{2+}:nucleotide ratio was much greater than 1:2. Two other distinct ENDOR features at 4.6 and 16.0 MHz were observed in both natural abundance and deuterated solvents. They are assigned to the ^{31}P nuclei of vanadyl bound nucleotides.[24] These two ENDOR features are separated by 11.4 MHz, which equals $2\nu_n$ for ^{31}P with $\mathbf{H}_0$ at 3270 G, and are centered about 10.3 MHz, which, thus, corresponds to $|A|/2$ for ^{31}P. This yields a hfc value for ^{31}P of 20.6 MHz. This value, which is dominated by isotropic inter-

(24) Equation 1 applies to the condition $\nu_n > |A|/2$. For the condition $\nu_n < |A|/2$, as applies here for the ^{31}P nucleus, the equation becomes $\nu_\pm = |A|/2 \pm \nu_n$.

Table III. Summary of Principal hfc Components and Estimated Metal–Proton Distances in VO^{2+}–Nucleotide Complexes[a]

$A_\parallel$	$A_\perp$	A_{iso}	$A_\parallel^D$	$A_\perp^D$	r (Å)	proton assignment
1.81	1.22	−0.21	2.02	−1.01	4.23	$-CH_2-$ (AMP-CP)
1.52	0.44	0.21	1.31	−0.65	4.88	$-CH_2-$ (AMP-CP)
1.07	0.44	0.06	1.01	−0.50	5.32	Ade:H(8) (ADP/AMP-CP)[b]
0.81	0.24	0.11	0.70	−0.35	6.02	Rib:H(5′) (ADP/AMP-CP)[b]
6.07	3.13	−0.06	6.13	−3.07	2.92	axial OH (Solvent)[c]
2.36	1.40	−0.15	2.51	−1.25	3.92	axial CH_3 (Solvent)[c]

[a] Hfc components are given in units of MHz. Estimated error in r is 0.1–0.2 Å. [b] The assignment of the H(8) and H(5′) protons is based on molecular modeling studies, as discussed in the text. [c] The parallel ENDOR features for these two solvent protons are observed in the −5/2 parallel spectrum (data not shown).

actions, is comparable to the value of 18.5 MHz estimated on the basis of the EPR superhyperfine structure. This value of through-bond, isotropic coupling for ^{31}P nuclei requires that the VO^{2+} ion is bound to the phosphate groups. A value of 8.5 G (23.8 MHz) for the hf coupling of ^{31}P has been reported for ternary complexes of *S*-adenosylmethionine synthetase with VO^{2+} and pyrophosphate or ATP.[25]

2. Analysis of ENDOR Splittings and Estimation of Metal–Proton Distances. From ENDOR spectra, two pairs of resonance features were identified for each class of protons, indicating that the hfc components for each class of protons exhibit axial symmetry. The experimentally observed ENDOR splittings arise predominantly from anisotropic dipolar interactions between the protons and the unpaired electron on the metal. There are also small isotropic interactions. These combine to give the observed hf couplings A, expressed in eq 2 as a function of electron–proton

$$A = g_e|\beta_e|g_N|\beta_N|(3\cos^2\phi - 1)/hr^3 + A_{iso} \qquad (2)$$

separation r and the dipolar angle ϕ. The other quantities in eq 2 have their classical definitions.[12]

In order to derive nuclear geometries from ENDOR spectra, it is necessary to determine the correspondence between observed ENDOR peaks and the direction of the molecule in the applied field. In this regard an incisive observation with respect to metal ion complexes of low g anisotropy is that the intense, well-resolved peaks observed at all applied magnetic field settings arise from protons in or near the x,y-plane of an axial complex.[26] On this basis, the ENDOR features tabulated in Table II and observed for both −5/2 parallel and −3/2 perpendicular field settings are directly assigned to perpendicular hfc components. Correspondingly, the resonance feature observed only with the −3/2 perpendicular applied field setting must correspond to the parallel hfc component. For protons in the x,y-plane of an axially symmetric complex, the observed parallel and perpendicular hf splittings correspond to values of $\phi = 0$ and 90°, respectively, in eq 2, and represent the principal hfc components $A_\parallel$ and $A_\perp$ of an axially symmetric hyperfine matrix. The dipolar hfc components $A_\parallel^D$ and $A_\perp^D$ can be determined from the observed splittings under the constraints $A_\parallel > 0 > A_\perp$ and $(A_\parallel + 2A_\perp) = 3A_{iso}$.[12] In Table III we have summarized our estimates of the principal dipolar and isotropic hfc components for each class of protons, along with the calculated metal–proton separations derived through application of the stratagem outlined above and applied in earlier studies.[12]

In Table III there are two classes of solvent protons that exhibit hf interactions with the VO^{2+} ion. These are ascribed to axially positioned methyl and hydroxyl protons. The ENDOR features from hydroxyl protons come either from water or methanol. In our previous ENDOR study of VO^{2+} in water–methanol cosolvent mixtures, we found two populations of VO^{2+} complexes in water–methanol mixtures, one with axially coordinated water and the other with axially coordinated methanol.[12] Both complexes had only water molecules coordinated in equatorial positions. On the basis of our identification of both axial methyl and hydroxyl protons, two such populations must also exist for VO^{2+}–nucleotide complexes with axially coordinated methanol or water in the inner coordination sphere.

The assignments of parallel and perpendicular hfc components are based on the stratagem outlined above for selective molecular orientation by choice of H_0 setting. For the $VO(AMP\text{-}CP)_2$ complex, the ENDOR determined values of the parallel and perpendicular hfc components of 1.81 and 1.22 MHz, respectively, yield an electron–proton separation of 4.23 Å for one methylene proton. From the hf couplings of 1.52 and 0.44 MHz assigned to the second methylene proton, the electron–proton distance is estimated as 4.88 Å. These values of r are listed in Table III. The alternative combination of the two principal hfc components, pairing 1.81 MHz with 0.44 MHz, and 1.52 MHz with 1.22 MHz, would have resulted in electron–proton distances of 4.67 and 4.37 Å, respectively. Although in both cases the electron–proton separations are similar, the isotropic contributions are much larger for the latter combination. Since these protons are approximately 5 Å distant from the metal center, we choose the combination of hf couplings that yield the smaller set of isotropic hf components, as listed in Table III. The same argument was also applied to the two protons assigned to the adenosine moiety, as listed in Table III.

The electron–proton separations in Table III were calculated according to eq 2 which is generally applicable for values of $r \geq 2.5$ Å under conditions of weak contact interactions.[27] For the VO^{2+} ion, the unpaired electron spin resides in the metal d_{xy} orbital. In a recent ENDOR study of a low-spin cyanide adduct of Fe^{3+}–transferrin, Snetsinger et al. demonstrated that short metal–proton distances of the order of 2.15 Å obtained by the classical point dipole approximation are in excellent agreement with the values calculated by explicitly using the integrated wave function of the ground-state d_{xy} orbital.[28] In our previous study of the solvation structure of the VO^{2+} ion, we have shown that for equatorially positioned, inner-sphere coordinated hydroxyl protons, the ENDOR determined distances of 2.5 and 2.6 Å were underestimated by ≤0.1 Å when compared to X-ray results.[12]

C. Molecular Modeling of Structures of the VO^{2+} Ion Complexed to Nucleotides. To deduce the coordination geometry of complexes of VO^{2+} with ADP and AMP-CP, as defined by our EPR and ENDOR results, we positioned the oxygen atom of the metal coordinated, axial solvent molecule so as to form a linear O···V═O configuration with metal–(hydroxyl) proton separations of 2.92 Å, in accord with the ENDOR results. The resultant axially coordinated oxygen atom is constrained to a position 2.23 Å distant from the vanadium, identical to the X-ray defined axial H_2O···V═O interaction of the pentaaquo vanadyl ion.[20] For the axial configuration of a metal-coordinated methanol molecule, the three methyl protons have separations of 3.92, 3.43, and 3.94 Å from the vanadium. In ENDOR spectra, two line pairs were observed for an axial methyl group yielding a 3.92 Å metal–proton separation, in excellent agreement with the model-based values.

We then established the geometry of the nucleotide coordination in the $VO(ADP)_2$ and $VO(AMP\text{-}CP)_2$ complexes as follows: (1) EPR spectrometric titrations showed that two nucleotide molecules bind to the VO^{2+} ion; (2) the EPR line width of the VO^{2+}–nu-

(25) (a) Markham, G. D. *Biochemistry* **1984**, *23*, 470–478. (b) Markham, G. D.; Leyh, T. S. *J. Am. Chem. Soc.* **1987**, *109*, 599–600.

(26) (a) Hurst, G. C.; Henderson, T. A.; Kreilick, R. W. *J. Am. Chem. Soc.* **1985**, *107*, 7294–7299. (b) Henderson, T. A.; Hurst, G. C.; Kreilick, R. W. *J. Am. Chem. Soc.* **1985**, *107*, 7299–7303.

(27) Schweiger, A. *Structure Bonding (Berlin)* **1982**, *51*, 1–128.

(28) Snetsinger, P. A.; Chasteen, N. D.; van Willigen, H. *J. Am. Chem. Soc.* **1990**, *112*, 8155–8160.

Table IV. Comparison of Dihedral Angles (deg) of the X-ray Defined Structures of Metal–Nucleotide Complexes and of the ENDOR Determined Structures of Complexes of VO^{2+} with ADP and AMP-CP

dihedral angle	X-ray			ENDOR[a]
	Na_2ATP[b]	$Mn(ATP)_2$[c]	$Rb(ADP)_2$[d]	
α[O(6′)–P(1)–O(5′)–C(5′)]	−52	−66	−59	−52 ± 10
β[P(1)–O(5′)–C(5′)–C(4′)]	136	171	147	−130 ± 10
γ[O(5′)–C(5′)–C(4′)–C(3′)]	49	55	57	35 ± 15
χ[O(4′)–C(1′)–N(9)–C(8)]	39	66	40	33 ± 10

[a] This work. [b] Reference 3a. [c] Reference 3b. [d] Reference 4.

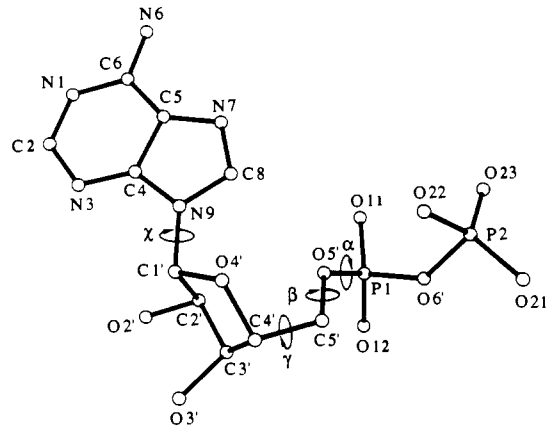

Figure 6. Illustration of the atomic numbering scheme for the ADP molecule and the four dihedral angles which characterize nucleotide conformation. The atomic numbering scheme is given according to the IUPAC-IUB joint commission on biochemical nomenclature.[30]

cleotide complexes was not influenced by introduction of perdeuterated solvents, indicating no equatorially bound solvent in the inner coordination sphere; (3) proton ENDOR spectra showed only axially coordinated solvent molecules and no evidence of equatorially bound solvent molecule; (4) the large isotropic hfc component for ^{31}P obtained from both EPR and ENDOR spectra indicated that the VO^{2+} ion binds to the pyrophosphate group of the nucleotides; and (5) EPR spectra of $VO(ADP)_2$ and $VO(AMP\text{-}CP)_2$ complexes showed a five-line superhyperfine pattern, indicating that all four phosphorus atoms in these complexes are equivalent with respect to vanadium. Therefore, we positioned the α and β phosphate groups of the two ADP or AMP-CP molecules in equatorial positions, so that the α and β phosphate oxygens of both molecules were coordinated to the VO^{2+} ion in a 2-fold symmetric manner.

Figure 6 illustrates the chemical bonding structure and atomic numbering scheme for ADP together with the four dihedral angles that characterize nucleotide conformation (cf., ref 29). The α and β phosphate oxygens in ADP are labeled O(11) and O(22), respectively. In the VO^{2+}–nucleotide complex, all four α and β phosphate oxygens were fixed in equatorial positions, so that the O=V—(equatorial) O angle is 97.9°.[12,20] This arrangement results in four structurally equivalent phosphorus atoms with respect to the vanadium. In the modeling studies we have found that the phosphorus atoms of the α and β phosphate groups in VO^{2+} complexes of both ADP and AMP-CP occupy structurally identical positions. Despite the difference in the P–C–P and P–O–P bond angles (117° and 135°, respectively), the P(1)···P(2) distances in both compounds are virtually identical due to different bond lengths for P–C (1.79 Å) and P–O (1.59 Å).[3a,18] In the $VO(AMP\text{-}CP)_2$ complex, the ENDOR determined metal–proton distances to the two methylene protons (4.23 and 4.88 Å) fix the positions of the α and β phosphate oxygen atoms through which both AMP-CP and ADP bind to VO^{2+}. The ENDOR constrained distances of these two methylene protons result in separations from the vanadium to the α and β phosphate oxygens of 2.32 Å and from the vanadium to the phosphorus atoms of 3.44 Å. This is in excellent agreement with the corresponding metal–nucleus distances in $Mn(ATP)_2$, as determined by X-ray diffraction studies.[3b]

After positioning the phosphate groups of AMP-CP or ADP, coordinated to the VO^{2+} ion in the equatorial positions, we then searched for plausible conformations of the adenosyl–ribose moiety that would account for the two proton ENDOR absorptions belonging to the nucleoside. This analysis was carried out on the basis of search calculations[17] of torsion angles around the C(1′)–N(9), C(5′)–C(4′), O(5′)–C(5′), and P(1)–O(5′) bonds.[30] The general methodology of the search calculations within the limits of nonbonded, hard-sphere interactions[17c] has been described previously.[19]

Assignments of the two ENDOR determined distances of 5.32 and 6.02 Å to only ribose protons were ruled out either because they resulted in energetically unfavorable structures with respect to the α and β dihedral angles[29] or because they would have required violations of van der Waals nonbonded contacts of the ribose moiety with phosphate oxygens or the vanadyl group. We then searched for sterically acceptable metal–proton distances, ascribing one to the ribose moiety and one to the purine base. There was no conformation acceptable with assignment of the 5.32-Å metal–proton distance to any ribose proton. However, with the nucleoside portion essentially in its X-ray defined conformation,[3a] the ENDOR determined metal–proton distances of 6.02 ± 0.20 and 5.32 ± 0.15 Å could be ascribed to the mean of the two H(5′) protons and the H(8) proton of the purine base, respectively. The resultant dihedral angles about the C(1′)–N(9), C(5′)–C(4′), C(5′)–O(5′), and P(1)–O(5′) bonds compatible with the ENDOR constraints are in excellent agreement with corresponding values obtained from X-ray diffraction studies of metal–nucleotide complexes, as summarized in Table IV. The structure of $[VO(AMP\text{-}CP)_2^{eq}(H_2O)^{ax}]$, as determined by EPR and ENDOR spectroscopy and molecular modeling, is illustrated in Figure 7.[31] The results of the ENDOR constrained search calculations show that (1) the base moiety has an *anti* conformation with respect to the glycosidic bond C(1′)–N(9) bond, (2) the conformation about the C(4′)–C(5′) bond is *gauche gauche*, and (3) the conformation about the C(5′)–O(5′) bond is *trans*.

An alternative ENDOR compatible structure could also be obtained by assignment of the 6.02 ± 0.20 Å metal–proton distance to the mean position of the H(5′) protons and by assignment of the 5.32 ± 0.15 Å distance to both the H(2′) and H(8) protons simultaneously. In this structure the resultant values of the α and β dihedral angles remained similar to those for the ENDOR values in Table IV while the value of γ was ca. −70°. Although this conformation is stereochemically acceptable and the dihedral angle γ can adopt three staggered conformations independent of the α and β dihedral angles,[29] we prefer the structural interpretation given in Figure 7 because we consider the assignment of the 5.32-Å distance simultaneously to the H(2′) and H(8) protons as physically unlikely.

Firstly, while the purine H(8) proton can adopt a metal–proton distance of 5.32 ± 0.15 Å with suitable rotation around the C(1′)–N(9) bond, the H(2′) proton is not equidistant and accounts

(29) Saenger, W. Structures and Conformational Properties of Bases, Furanose Sugars, and Phosphate Groups. In *Principles of Nucleic Acid Structure*; Cantor, C. R., Ed.; Springer-Verlag: New York, 1984; Chapter 4, pp 51–104.

(30) Abbreviations and symbols for the description of conformations of nucleotides are given in accord with the IUPAC-IUB Joint Commission on Biochemical Nomenclature. *Eur. J. Biochem.* **1983**, *131*, 9–15.

(31) A listing of molecular-graphics-derived atomic coordinates of the complex illustrated in Figure 7 will be provided upon written request.

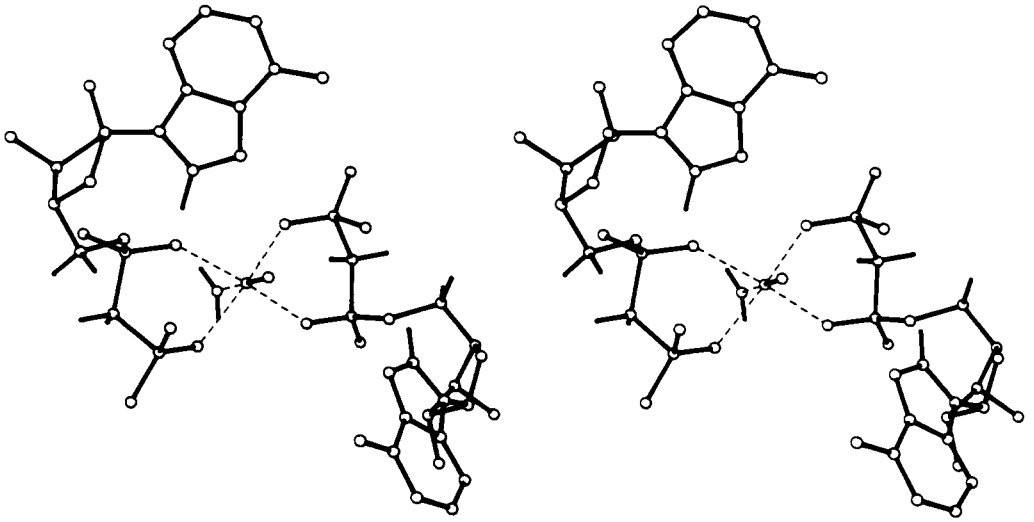

Figure 7. Stereodiagram of $[VO(AMP\text{-}CP)_2^{eq}(H_2O)^{ax}]$ determined on the basis of EPR and ENDOR spectroscopy and molecular modeling. Broken lines connect the vanadium both to the α and β phosphate oxygens of the two symmetry-related, equatorially-positioned AMP-CP molecules and to the axial water molecule. The ENDOR determined hydrogen atom positions of the two methylene protons, H(8) and H(5′), and the axially coordinated water protons are shown in addition to the non-hydrogen atoms.

for this value of r only through the uncertainty of ±0.15 Å; and the line width of the resonance is not unusually broad compared to other resonance features. Secondly, we expect the contribution of the H(2′) proton to the ENDOR spectrum to be diminished with respect to that of the H(8) proton because of structural disorder in the ribose ring. In solution, nucleotides are known to undergo a rapid conformational interconversion of the ribose ring involving displacement (puckering) of the C(3′) and C(2′) atoms from a mean plane.[29] In frozen solution, the corresponding positions of the H(2′) and H(3′) protons are consequently disordered with respect to the metal ion because of the multiple conformations of the ribose ring. Since structural disorder diminishes the contribution of a proton to its peak-to-peak resonance amplitude, as observed, for instance, by comparison of the resonances of the ring protons in saturated and unsaturated five-membered nitroxyl spin-labels,[32] we believe that the ribose H(2′) proton does not contribute significantly to the observed ENDOR spectra.

In Figure 7 the adenine base has an *anti* conformation with respect to the dihedral angle χ. We have paid particular attention through modeling studies to the question of whether an *anti* conformation best accommodates the ENDOR results since both *syn* and *anti* conformations of purine nucleotides can exist in solution.[29] To this end we assigned to H(2) the ENDOR determined distance of 5.32 ± 0.15 Å and carried out two torsion angle search calculations. In the first case, we also applied the distance constraint of 6.02 ± 0.20 Å to H(5′). No conformation was found compatible with these constraints to both H(2) and H(5′). In the second search calculation, no other distance constraint besides the one for H(2) was used. In this case, we did find a conformation compatible with this ENDOR distance having dihedral angles χ of 140 ± 10°, γ of 120 ± 20°, and β of 185 ± 15°. In this conformation, electron–proton distances for the two amine protons of the N(6) of adenine would be in the range of 5.0–5.8 Å. We rule against this interpretation because we did not observe ENDOR features attributable to the amine protons in natural abundance solvents, as we should have if they indeed were 5–6 Å distant from the vanadium nucleus. Moreover, this conformer had a fully eclipsed conformation about the C(4′)–C(5′) bond. Therefore, it should be higher in energy relative to the staggered conformers around the γ dihedral angle. From free energy conformational maps of nucleosides, Pearlman and Kollman have shown that for χ the global energy minimum corresponds to an *anti* conformation while the second minimum corresponds to the *syn* conformation.[33] They have also shown that for the dihedral angle γ there are three staggered minima which are about 4 kcal/mol lower in energy than that of the eclipsed structures. On this basis, we rule against a *syn* conformation of the glycosidic bond and conclude that in $VO(ADP)_2$ and $VO(AMP\text{-}CP)_2$ the base exhibits an *anti* conformation with respect to the ribose ring.

D. General Conclusions. This study has demonstrated the advantage of using VO^{2+} as an EPR and ENDOR probe for structural characterization of metal complexes in solution. In the present study with VO^{2+}–nucleotide complexes, we have established the metal binding sites, the stoichiometry of metal:ligand binding, and the molecular geometry of the metal–nucleotide complexes in solution. Although on the basis of ^{17}O NMR studies of Mn^{2+}–ADP complexes in solution it has been postulated that the $Mn(ADP)_2$ species exists in solution,[5a] no direct evidence was found. The present study provides for the first time direct structural evidence that with ADP, AMP-CP, and ATP, $[VO(nucleotide)_2^{eq}(solvent)^{ax}]$ species are formed in solution. For ADP and AMP-CP complexes, VO^{2+} is chelated via the α and β phosphate groups. The conformation of the VO^{2+}-bound nucleotide that best accommodates the ENDOR determined metal–proton distances within hard-sphere limits is essentially identical to that defined by X-ray studies for other metal–adenosine nucleotide complexes in crystals.[3a,b,4]

For ATP, chelation must occur via the terminal β and γ phosphate groups. This binding geometry places the VO^{2+} ion further from nucleoside protons of the ATP moiety, consistent with their absence in ENDOR spectra of $VO(ATP)_2$. On the other hand, studies of the VO^{2+} ion complexed to methylene analogues of ATP under conditions of neutral pH show very low affinity of binding and very different binding stoichiometry. These analogues are used as substrate probes of protein–nucleotide interactions and are assumed to be structurally isomorphous with ATP. Our studies have demonstrated that in these complexes near pH 7 the metal binding characteristics and metal:ligand stoichiometry are different, indicating that they do not exhibit complete isomorphous behavior to that of ATP.

(32) Mustafi, D.; Wells, G. B.; Joela, H.; Makinen, M. W. *Free Radical Res. Commun.* **1990**, *10*, 95–101.

(33) Pearlman, D. A.; Kollman, P. A. *J. Am. Chem. Soc.* **1991**, *113*, 7167–7177.